Fusion Experiments of HSI and High Resolution Panchromatic Imagery[1]

Su May Hsu[2] and Hsiao-hua Burke
MIT Lincoln Laboratory
244 Wood Street, Lexington, MA 02420-9185

Abstract

In this paper, the fusion of hyperspectral imaging (HSI) sensor data and high-resolution panchromatic imagery (HPI) is explored. Spatial/spectral sharpening techniques have been proposed to increase the spatial resolution of spectral imagery with HPI. The intent of the process is to reconstruct high spatial resolution imagery with high spectral fidelity. Target detection and identification of such imagery can be achieved with spectral and spatial processing techniques.

Three sharpening approaches are reviewed here. The first one uses pseudo-inverse techniques, the second and third are component replacement methods in spatial and frequency domains, respectively. The performance of these approaches are assessed and shown with examples. In addition, a spatial-spectral analysis with fusion of HSI and HPI is also demonstrated for enhanced target detection and identification.

1 Introduction

Conventional single band or multi-spectral sensors typically image in wide, discrete spectral bands with fine spatial resolutions. In contrast, hyperspectral imaging sensors collect image data in hundreds of contiguous, narrow spectral bands (~10 nm) with coarser resolutions. The increased number of sensor bands provides higher spectral resolution and more opportunities to detect subtle spectral differences in signatures that are too narrow to be differentiated in multi-spectral imagery. For each ground sample distance (GSD) pixel within a hyperspectral image, a continuous spectrum is measured and used to identify materials by their reflectance or emissivity. On the other hand, signal-to-noise ratios (SNR) of the HSI data tend to be sub-optimal. To maintain certain SNR, HSI resolutions are in general coarser than broadband image resolutions. If hyperspectral image can be spatially "sharpened" via the broadband high-resolution image, the overall performance is expected to improve further.

---

[1] This work was sponsored by the Department of Defense under Air Force Contract F19628-95-C-0002. Opinions, interpretations, conclusions and recommendations are those of the authors and not necessarily endorsed by the United States Air Force.

[2] Telephone (781) 981-2920; Fax (781) 981-7271; e-mail sumayhsu@ll.mit.edu

REPORT DOCUMENTATION PAGE

Form Approved OMB No. 0704-0188

1. REPORT DATE (DD-MM-YYYY)	2. REPORT TYPE	3. DATES COVERED (FROM - TO)
01-01-2001	Conference Proceedings	xx-xx-2000 to xx-xx-2000

4. TITLE AND SUBTITLE
Fusion Experiments of HSI and High Resolution Panchromatic Imagery
Unclassified

5a. CONTRACT NUMBER
5b. GRANT NUMBER
5c. PROGRAM ELEMENT NUMBER

6. AUTHOR(S)
Hsu, Su May ;
Burke, Hsiao-hua ;

5d. PROJECT NUMBER
5e. TASK NUMBER
5f. WORK UNIT NUMBER

7. PERFORMING ORGANIZATION NAME AND ADDRESS
MIT Lincoln Laboratory
244 Wood Street
Lexington, MA02420-9185

8. PERFORMING ORGANIZATION REPORT NUMBER

9. SPONSORING/MONITORING AGENCY NAME AND ADDRESS
Director, CECOM RDEC
Night Vision and Electronic Sensors Directorate Security Team
10221 Burbeck Road
Ft. Belvoir, VA22060-5806

10. SPONSOR/MONITOR'S ACRONYM(S)
11. SPONSOR/MONITOR'S REPORT NUMBER(S)

12. DISTRIBUTION/AVAILABILITY STATEMENT
APUBLIC RELEASE
,

13. SUPPLEMENTARY NOTES
See Also ADM201258, 2000 MSS Proceedings on CD-ROM, January 2001.

14. ABSTRACT
In this paper, the fusion of hyperspectral imaging (HSI) sensor data and high-resolution panchromatic imagery (HPI) is explored. Spatial/spectral sharpening techniques have been proposed to increase the spatial resolution of spectral imagery with HPI. The intent of the process is to reconstruct high spatial resolution imagery with high spectral fidelity. Target detection and identification of such imagery can be achieved with spectral and spatial processing techniques. Three sharpening approaches are reviewed here. The first one uses pseudo-inverse techniques, the second and third are component replacement methods in spatial and frequency domains, respectively. The performance of these approaches are assessed and shown with examples. In addition, a spatial-spectral analysis with fusion of HSI and HPI is also demonstrated for enhanced target detection and identification.

15. SUBJECT TERMS

16. SECURITY CLASSIFICATION OF:			17. LIMITATION OF ABSTRACT	18. NUMBER OF PAGES	19. NAME OF RESPONSIBLE PERSON
a. REPORT	b. ABSTRACT	c. THIS PAGE	Public Release	10	Fenster, Lynn lfenster@dtic.mil
Unclassified	Unclassified	Unclassified			19b. TELEPHONE NUMBER International Area Code Area Code Telephone Number 703767-9007 DSN 427-9007

Currently, there are a number of space-based hyperspectral measurement platforms to be launched in the foreseeable future: NASA's EO-1, Air Force's Warfighter-1 and Navy's NEMO (Naval Earth Map Observer). Their characteristics are summarized in Table 1. Note that in addition to the HSI sensor, a high-resolution panchromatic imaging (HPI) sensor is also onboard for each of these systems, with the linear spatial resolution of 3 to 8 times better. It is important that effective approaches of hyperspectral image sharpening with the high-resolution broadband image be explored to enhance the utility of future HSI data.

A number of approaches have been attempted and applied to multi-spectral images. In Section 2, three approaches are briefly reviewed and implemented: the pseudo-inverse technique, color normalization, and spatial frequency correction methods. Enhanced target detection and identification is illustrated in Section 3 with additional spatial-spectral analysis of fusion of high-resolution information.

2 Review and Demonstration of Sharpening Approaches

In this section, three techniques for image sharpening are first reviewed. A sample data is created based on field data. The algorithms are then applied to the generated HSI and HPI data for a sharpened HSI. Algorithm performance is then evaluated by comparing with the original truth data.

2.1 Approaches

Three sharpening approaches discussed here are: pseudo-inverse techniques, and component replacement methods in spatial and frequency domains, respectively.

2.1.1 Pseudo-inverse technique [1, 2]

Given a high-resolution panchromatic image (HPI) co-registered with a set of hyperspectral images, a system of equations can be established for the reconstruction of a high spatial resolution HSI (SHSI). The value at a pixel in HPI is the spectral sum at the same pixel in SHSI and the spectral value at a pixel in HSI is the pixel-sum over the HSI GSD in the same spectral band of SHSI. If the sharpening ratio is r and the number of spectral bands is b, then the number of equations over the GSD of HSI is $r^2 + b$, and the number of unknowns for the SHSI reconstruction is $r^2 \times b$. As the sharpening ratio and the number of spectral band increase, the number of unknowns increases faster than the number of additional equations. The system of equations is under determined for a unique solution. Pseudo matrix inversion algorithms are applied to obtain a solution with least-mean-squared (LMS) estimations for the fusion problem. In this approach, it is important that the panchromatic image is in perfect registration with HSI. The pseudo inverse technique requires singular value decomposition. In addition, the LMS estimations based on the under determined system of equations may not achieve the required spectral accuracy.

2.1.2 Color Normalization

The color normalization algorithm conventionally used in MSI [3] is modified for HSI sharpening. It multiplies each of the HSI bands by the HPI and the resulting values are each normalized by the averaged HPI data over the number of pixels equivalent to the GSD of HSI. It is defined by the following equation:

$$\mathbf{SCN_i = (HSI_i * HPI) / ave(HPI)_{GSD}}$$

where HSI_i is the HSI band and SCN_i is the sharpened image band by color normalization.

The approach is straightforward in merging the spatial contrast of HPI into each spectral band of HSI. Similar to the pseudo-inverse technique approach, it also requires precise HSI/HPI registration and the reconstructed data may not achieve great spectral accuracy.

2.1.3 Spatial Frequency Correction

Some sharpening approaches use wavelet transformations[4]. Images are decomposed into different spatial frequency scales. For each of the HSI bands, the high frequency components are replaced with components from HPI. The sharpened image is then obtained via inverse transformation of the modified spectra. In practice, 2-D Fourier transformation can be applied for image spatial frequency analysis. The sharpening process is described as below:

$$\mathbf{SFC_i = FFT^{-1}\{FFT\,(HSI_i)_{low} + FFT(HPI)_{hi}\}}$$

where SFC_i is sharpened HSI_i by frequency correction, $FFT\,(HSI_i)_{low}$ represents low frequency components of HSI_i and $FFT(HPI)_{hi}$ represents high frequency components of HPI

In this approach, the spatial shift due to imperfect HSI/HPI registration will show up as a phase shift in the frequency spectrum. In addition, careful selection of the number of high frequency components for replacement is required to avoid artifacts in the sharpened image. Once again, some loss of spectral quality is expected in the reconstructed data.

2.2 Demonstration Example

The review in Section 2.1 indicates that all three approaches require good co-registration between HSI and HPI. Since HSI and HPI commonly co-exist on the same platform, co-registration to within a small fraction of an HPI pixel is expected. For performance comparisons, perfect co-registration is assumed here. Future work will address the co-registration issues. A set of simultaneous HSI and HPI data is generated and applied with the sharpening methods. A HYDICE (Hyperspectral Digital Image Collection Experiment) major frame is used as the "truth" in both spatial (0.8 m/pixel) and spectral ($\Delta\lambda \sim 10$ nm) domains. This input "truth" data is then processed to generate the

contemporaneous test data of HSI (8 m/pixel, $\Delta\lambda \sim 10$ nm) and HPI (0.8 m/pixel, wide band). The first major frame of HYDICE data from Forest Radiance I Run 05 is used. The frame is a portion of a forest scene. It contains camouflage nets (> 10 m x 10 m) and several vehicles (~ 4 m x 8 m). The image has 320x320 pixels, 0.8 m per pixel. 25 bands from 0.63 μm to 0.9 μm are used. The HPI data is generated with a 25-band integration. It is a 320x320 single-band image with 0.8 m per pixel. The HSI data for test is obtained by under-sampling the spatially blurred input data. The FWHM (full width half maximum) of the blurring point spread function (PSF) is 5-pixel wide and the spatial under-sampling is 5 to 1. The resulting HSI has 25 bands; each band is 64 x 64 pixels in size and 4 m per pixel. Figure 1 depicts the flow of data generation for HSI and HPI fusion.

Results of sharpening using the three approaches are shown in Figure 2. All three images are visually sharper than the low resolution HSI and comparable to the original input of HSI ("the truth"). Two measures, spectral angle and spectral distance (Euclidean distance), are used to evaluate the sharpening algorithms. These are calculated as:

$$\textbf{Spectral Angle (A,B)} = \cos^{-1}(A \cdot B / |A|\,|B|)$$

$$\textbf{Spectral Distance (A,B)} = |A - B|$$

where, A and B are two multi-band spectra.

A zero angle and zero distance represent a perfect match of the two spectra. The sharpened images are compared to "the truth" data in terms of spectral angle and spectral distance. The spectral distance normalized by the pixel amplitude in the truth image is calculated for comparison. The frame-averaged differences are listed in Table 2. For comparison, the difference measurements from the unsharpened HSI are also included in the table. It shows that the sharpened images improve significantly from the unsharpened HSI in spectral distance, but shows no obvious improvement in spectral angle. Among the sharpened images, color normalization (SCN) is closer to the truth in spectral angle than results of pseudo-inverse (SPI) and frequency correction (SFC). On the other hand, the image of frequency correction is the closest to the truth in spectral distance.

The sharpened images generally appear spatially sharper. However, the impact of such results on target detection and identification is small. Since the combined HSI and HPI data is severely under-determined, spectral features of objects smaller than the original HSI resolution cannot be fully resolved in the reconstruction of the sharpened HSI. For enhanced target detection and identification, additional spatial and spectral analysis at feature level, as discussed below, is necessary. In this paper, sharpened HSI image by color normalization will be used for further analysis.

3 Spatial-spectral Analysis

Various spatial and spectral analysis approaches have been attempted [5,6,7]. Here, a combined spatial-spectral analysis is carried out to demonstrate HSI and HPI fusion for

enhanced background characterization and target detection/identification. An analysis approach is depicted in Figure 3. The HSI data is first applied with background classification and anomaly detection. The background class statistics calculated from HSI are employed when the sharpened HSI is also processed with background classification and target detection. At the same time, spatial edge detection for target and background boundaries is applied to the HPI. These edges are combined with results from the sharpened HSI. Targets and backgrounds are spatially defined by the edges. Subsequently, their materials can be identified with spectral characteristics.

In order to evaluate the analysis performance, an expanded data set is used here. Three major frames of HYDICE data from Forest Radiance I Run 05 are used in the demonstration example. The original image of 300x960 pixels in size, 0.8 m per pixel and 210 bands (the "truth" image) is used as the input. The simulated low-resolution HSI is 60x192 pixels in size, 4 m per pixel and 210 bands. The HPI is obtained with band integration from 0.4 to 0.8 μm, 300x960 pixels with 0.8 m per pixel. A sharpened HSI data cube is constructed from the HSI and HPI with the color normalization method.

Figure 4 shows a reference image (RGB) of HSI, as well as background classification and anomaly detection map derived from the unsharpened HSI. The classification is performed with an unsupervised feature extraction using principal component analysis (PCA). The Eigen space is first determined for the scene from the covariance matrix of the data cube. It then divides the scene into classes of maximal separations in the Eigen space. In the 5-class classification shown here, road, vegetation (bright and dark), shade and ground are delineated in the scene. The background map and spectral statistics of these classes from HSI are employed in all subsequent processing. Anomalies distinct from backgrounds are also detected. These detections are used to cue for target detection and identification in the combined analysis. Edges detected from HPI with a SOBEL[8] operator are shown in Figure 5. Overlay of the edges with background classification from sharpened HSI is also shown in the figure. Background boundaries in the sharpened HSI are better defined than in the unsharpened HSI. These boundaries are further enhanced with the edges derived from HPI. The image on the right of Figure 5 depicts the combined results of spectral matched filtering and spatial edges over regions with anomaly detections from HSI. Red and green portions each represent the detection of different vehicle paints. The detections are in general bounded by the edges shown in blue. However, two regions of detection located at the top of the scene are not well defined in shape and appear to be large in size. These are inconsistent with features of vehicles. Further testing with spectral matched filtering with two types of fabric confirms and identifies pieces of fabric in these regions as shown in the leftmost image of Figure 6. An enlarged view of the vehicle detections is also shown in the figure. The vehicle size and orientation can be determined from the bounding edges. It is classified as large (4x8 m^2) in size if it is 4 to 7 pixels wide and 8 to 11 pixels long or as small (3x6 m^2) in size if it is 3 to 5 pixels wide and 6 to 7 pixels long. The colored bar next to each vehicle in the enlarged image depicts its type of paint, size and orientation.

4 Summary

In this paper, sharpening approaches were investigated and implemented on a combined HSI and HPI data set. The sharpened HSI retained the spectral signatures of extended area in HSI and in general appeared spatially sharper. However, spectral features of objects smaller than the original HSI resolution were not fully resolved through sharpening due to the under-determined nature of the combined data set. Further spatial and spectral analysis was then demonstrated to combine high-resolution information from HSI and HPI for enhanced background characterization and target detection and identification. Anomalies distinct from backgrounds were also detected from HSI and used to cue for target detection and identification in the combined analysis. Spatial image processing was applied to HPI for edge analysis. As a result of combined analysis, specific target material, size and shape were determined.

References

1. Tim J. Patterson, Michael E. Bullock, "Radiometrically Correct Sharpening of Multispectral Images using a Panchromatic Image", p. 252-264, SPIE Vol.2234
2. Tim J. Patterson, Lester Gong, Robert Haxton, Troy Chinen, "Extension of Sharpening Techniques to Hyperspectral Data", P. 114-122, SPIE Vol.3372, April 1998
3. Jim Vrabel, "Advanced Band Sharpening Study", p. 73-84, SPIE Vol.3071, April, 1997
4. Mark A. Goforth, "Multispectral Image Sharpening with Multiresolution Analysis and the MTF", P. 123-131, SPIE Vol.3372, April 1998
5. Harry N. Gross, John R. Schott, "Application of Spatial Resolution Enhancement and Spectral Mixture Analysis to Hyperspectral Images", P. 30-41, SPIE Vol.2821, 1996
6. Harry N. Gross, John R. Schott, "Application of Spectral Mixture Analysis and Image Fusion Techniques for Image Sharpening", P.85-94, Remote Sensing and Environment 63, 1998
7. Bing Zhang, Jiangui Liu, Xiangjun Wang, Changshan Wu, "Study on the Classification of Hyperspectral Data in Urban Area", P. 169-172, SPIE Vol.3502
8. R. C. Gonzalez, P. Wintz, Digital Image Processing, Addison-Wesley, 1987

Table 1 Future Space-based Hyperspectral Measurement Platforms

Sensor	EO-1 (NASA)	Warfighter-1 (Air Force)	NEMO (Navy)
HSI Spectral	0.4 - 2.5 μm, 220 bands	0.4 - 2.5 μm, 200 bands	0.4 - 2.5 μm, 210 bands
HSI IFOV	30 m	8 m	30 m
Scene Size	7.5 km x 100 km	5 km x 20 km	30 km x 200 km
Co-incident HPI	10 m	1 m	5 m
Launch	2000	2001	~2001

Table 2 Sharpening Algorithm Performance

Average spectral angle and distance over 1st major frame of HYDICE Forest Radiance I Run 05

Performance Metrics	Unsharpened HSI	Sharpened		
		Pseudo Inverse	Frequency Correction	Color Normalization
Spectral Angle $\cos^{-1}(X \cdot M_i / \lvert X \rvert \lvert M_i \rvert)$	4.9^o	8.3^o	5.8^o	3.8^o
Spectral Distance* $(X - M_i)^T (X - M_i)$	21.6%	13.8%	8.2%	10.0%

* Spectral Distance normalized to the pixel amplitude in the "truth" image

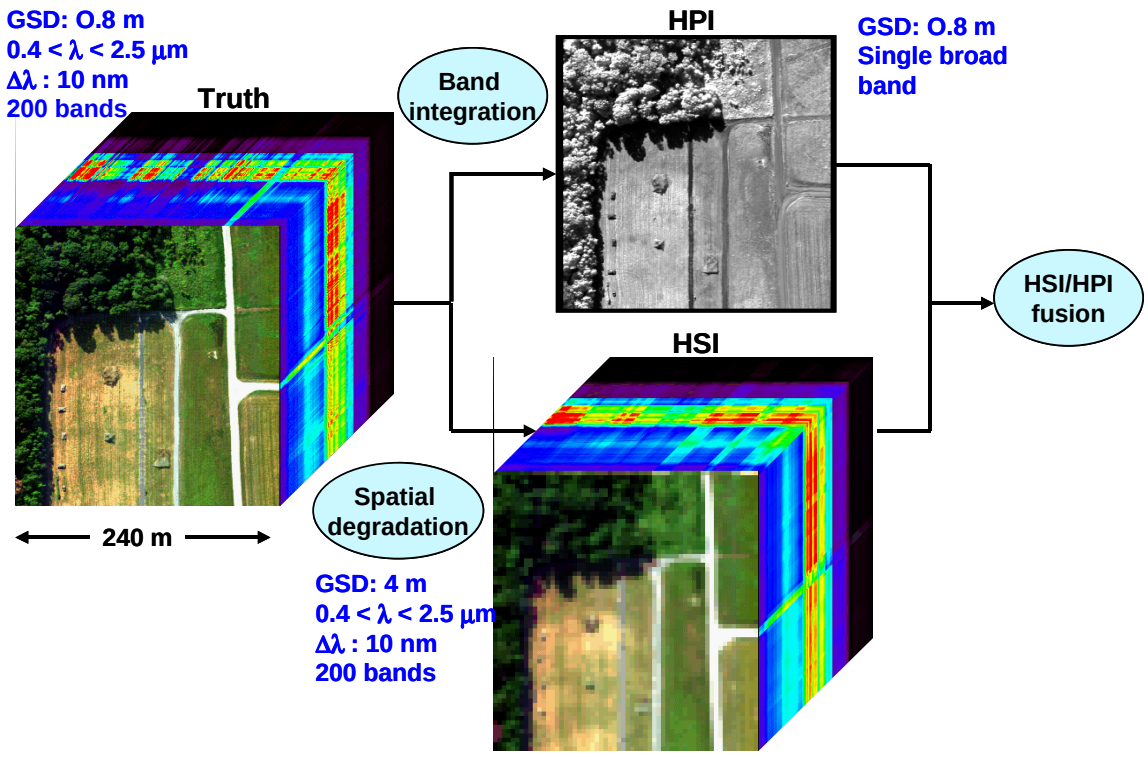

Figure 1 Flow diagram of data generation for HSI and HPI fusion

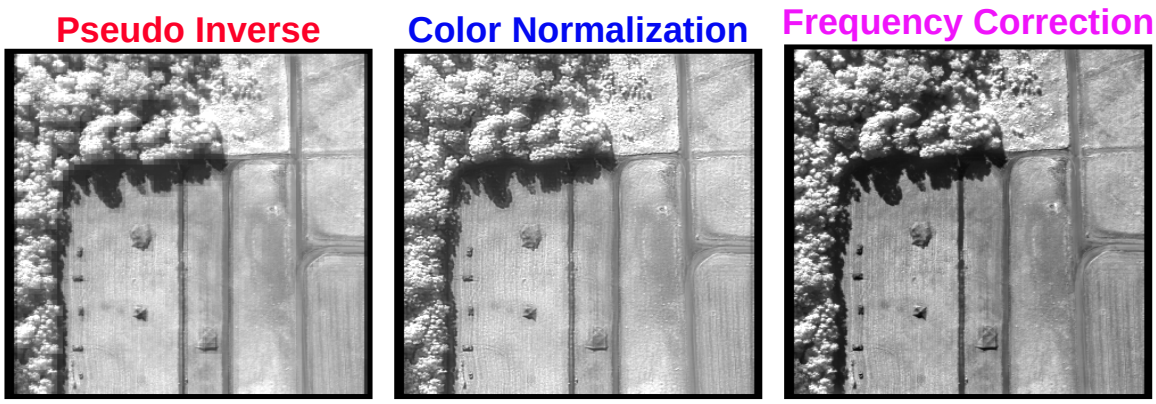

Figure 2 The sharpened images by pseudo inverse, color normalization and frequency correction are shown at 0.75 μm

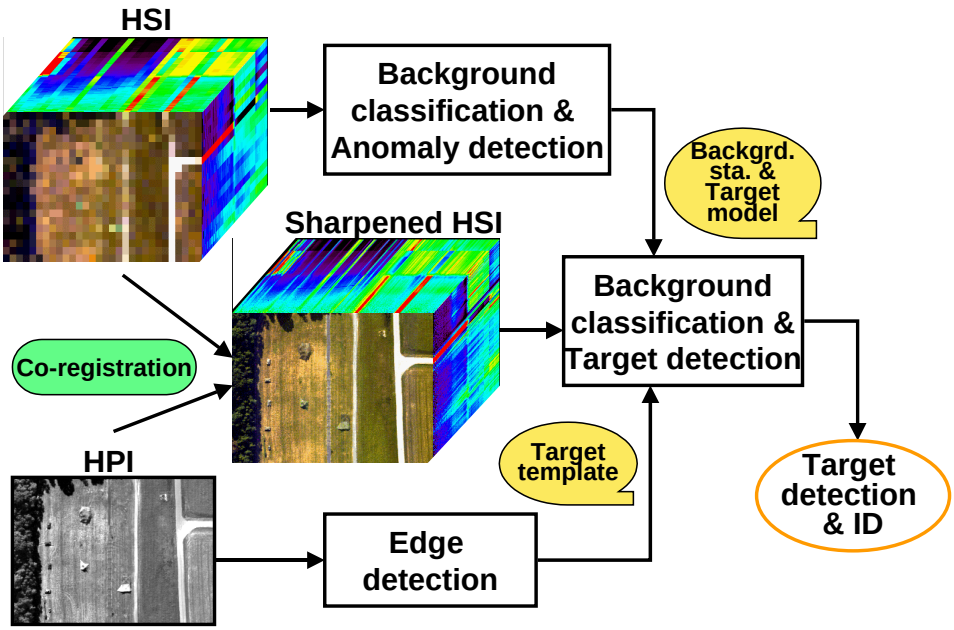

Figure 3 A Spatial-spectral analysis approach

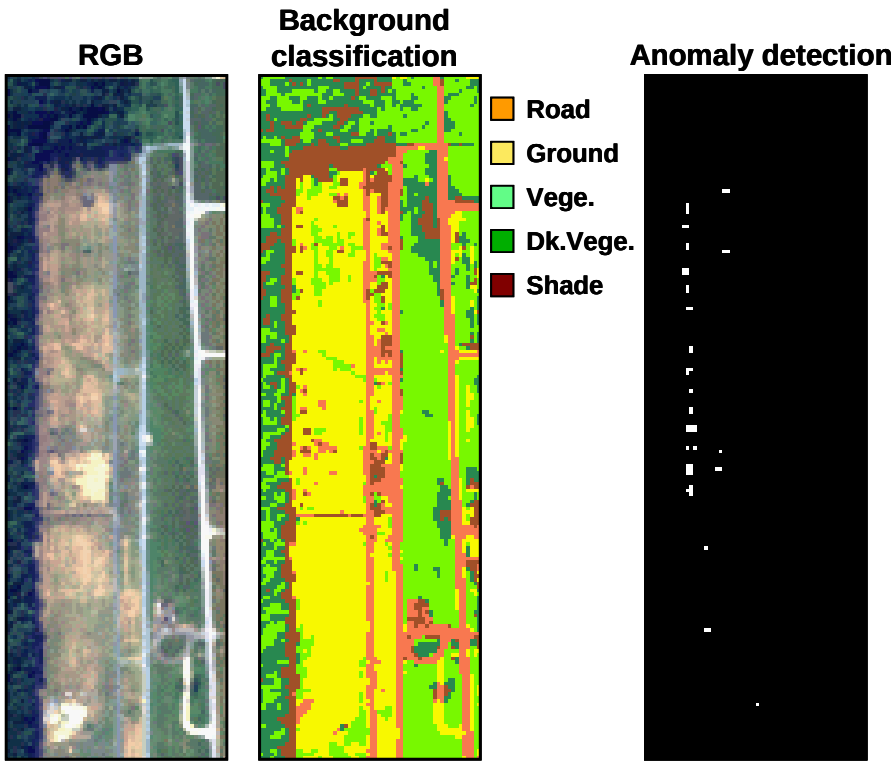

Figure 4 RGB image of HSI, background classification and anomaly detection derived also from the unsharpened HSI

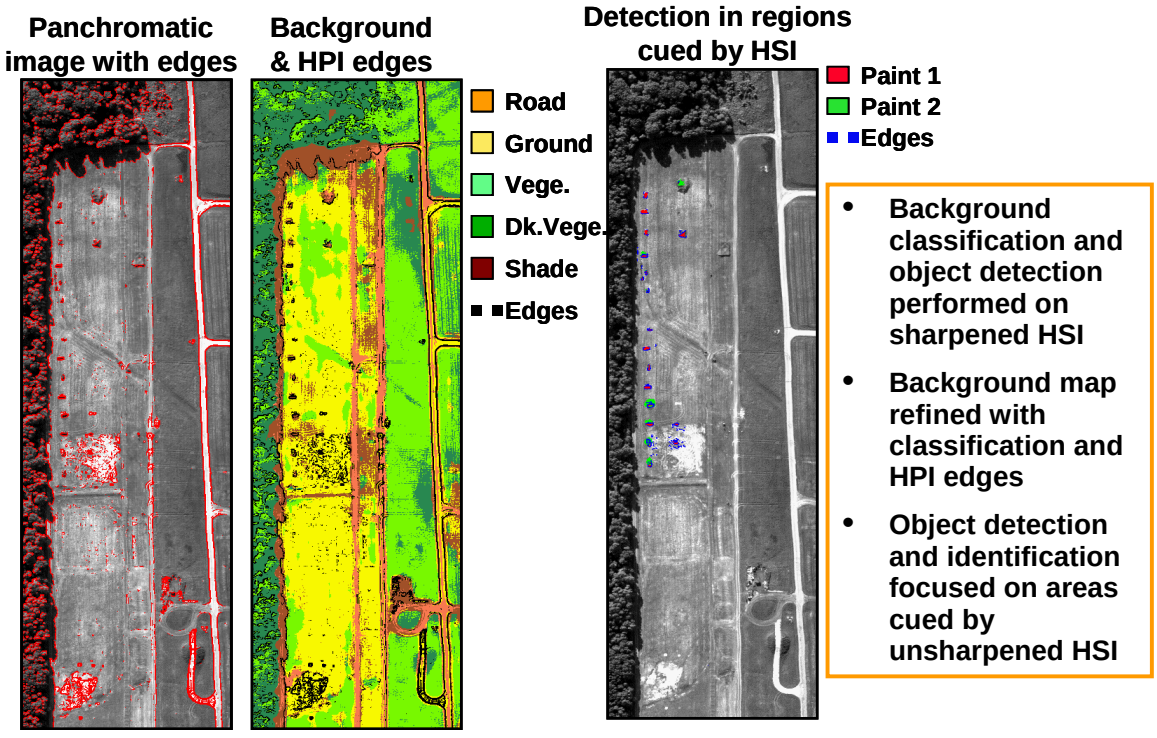

Figure 5 Edge detection on HPI, background classification and target detection on sharpened HSI

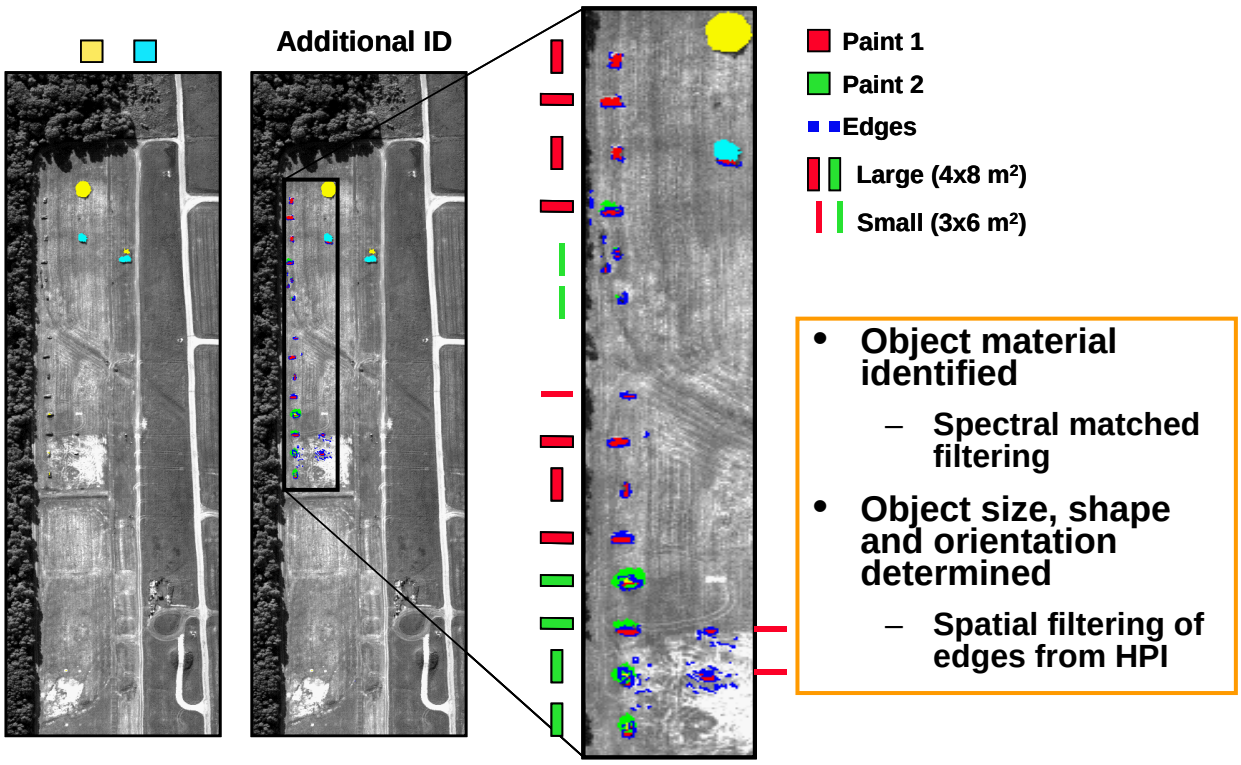

Figure 6 Fabric and additional object identification